HHS Public Access

Author manuscript

Nat Neurosci. Author manuscript; available in PMC 2011 January 01.

Published in final edited form as:

Nat Neurosci. 2010 July ; 13(7): 897–905. doi:10.1038/nn.2580.

In situ visualization and dynamics of newly synthesized proteins in rat hippocampal neurons

Daniela C. Dieterich[1,2], **Jennifer J.L. Hodas**[1], **Geraldine Gouzer**[3], **Ilya Y. Shadrin**[1], **John T. Ngo**[4], **Antoine Triller**[3], **David A. Tirrell**[4], and **Erin M. Schuman**[1,5]

[1]Division of Biology, California Institute of Technology, Pasadena, CA, USA

[2]Leibniz-Institute for Neurobiology, Magdeburg, Germany

[3]Institut de Biologie de l"Ecole Normale Supérieure (IBENS), Inserm U1024, CNRS UMR8197, 75005 Paris,France

[4]Division of Chemistry and Chemical Engineering, California Institute of Technology, Pasadena, CA, USA

[5]Max Planck Institute for Brain Research, Frankfurt, Germany

Abstract

Protein translation has been implicated in different forms of synaptic plasticity but direct *in situ* visualization of new proteins is limited to one or two proteins at a time. Here we describe a metabolic labeling approach based upon incorporation of non-canonical amino acids into proteins followed by chemo–selective fluorescent tagging via click chemistry. Following brief incubation with azidohomoalanine or homopropargylglycine, a robust fluorescent signal was detected in somata and dendrites. Pulse–chase–like application of azidohomoalanine and homopropargylglycine allowed visualization of proteins synthesized in two sequential time periods. This technique can be used to detect changes in protein synthesis and to evaluate the fate of proteins synthesized in different cellular compartments. Moreover, using strain–promoted cycloaddition, we explored the dynamics of newly synthesized membrane proteins using single particle tracking and quantum dots. The newly synthesized proteins exhibited a broad range of diffusive behaviors as expected if the pool of labeled proteins was heterogeneous.

Introduction

The visualization of a newly synthesized proteome has been hindered so far by the fact that proteins, new and old, share the same pool of amino acids and thus are chemically

Author Contributions D.C.D., J.J.L.H., G.G., and E.M.S. performed experiments; D.C .D., G.G. A.T. and E.M.S. designed experiments; D.C.D., J.J.L.H.,I.Y.S., G.G. and E.M.S. analyzed data; D.C.D., G.G., A.T. and E.M.S. wrote the paper; J.T.N. and D.A.T. provided reagents.

Note: Supplementary information for this article is available on the Nature Neuroscience website.

Competing interests statement

The authors declare no competing financial interests.

indistinguishable. Radioisotopic amino acids can provide potent labeling of newly synthesized proteins but the subsequent visualization of new proteomes in intact cells is not well–resolved or amenable to current fluorescence microscopy techniques.

The proteome of a neuron is a dynamic entity – tightly regulated by protein synthesis and degradation to maintain homeostasis or to adapt to changing environmental conditions. Many studies of behavioral and synaptic plasticity have demonstrated that long–lasting changes in synaptic transmission and behavior require both gene transcription and mRNA translation (reviewed in ref.1). Indeed, a distinguishing feature of late–phase long–term potentiation is that it requires both gene transcription and mRNA translation (e.g. ref.2). Protein synthesis occurs in somata, as well as in the protrusions of neurons and other polarized cells. In neurons, there is abundant evidence from both *in vivo* and *in vitro* experiments that dendritic protein synthesis is used to allow neuronal synapses to respond dynamically and in a specifically local way to the stimulation patterns that drive the establishment, maintenance and plasticity of synaptic connections3–6. Moreover, several studies have demonstrated that different biochemical fractions, which lack somatic protein synthesis machinery are nonetheless capable of synthesizing proteins (see refs.7, 8 for review), and several proteomics studies have identified proteins belonging to different functional classes9–11. Despite overwhelming support for the general notion of dendritic protein translation in plasticity and synaptic function, local protein translation has been monitored so far for only a few candidate proteins. Visualization of newly synthesized proteins in neurons has largely relied on the use of green fluorescent protein GFP– either as a fusion with the protein of interest or with the coding sequence for GFP flanked by the 5' and 3' UTRs (to confer regulation of mRNA translation) of the protein of interest12–14 – or a protease–controlled tag15. All of these approaches require over–expression of the coding sequence and/or the regulatory regions of the mRNA. The ability to visualize the pool of newly synthesized endogenous proteins has been hampered by the fact that all proteins share the same pool of 20 amino acids. However, recent work16–19 has expanded the natural repertoire of amino acids and introduced small, bioorthogonal groups that are metabolically incorporated into nascent proteins, enabling one to pulse label a set of new proteins20.

We recently described the use of the azide–bearing amino acid azidohomoalanine (AHA) or the alkyne–bearing amino acid homopropargylglycine (HPG) for incorporation into new proteins by making use of the cell's own protein synthesis machinery; this technology is called BONCAT, BioOrthogonal Non–Canonical Amino acid Tagging21,22). In BONCAT the methionine surrogate AHA is incorporated into newly synthesized proteins at methionine codons and subsequently tagged with an alkyne–affinity tag via copper–catalyzed azide–alkyne [3+2] cycloaddition (CuAAC;23) for the ultimate identification of AHA–labeled proteins using mass spectrometry. Here, we introduce, using a new generation of fluorescent tags, a sister technology to BONCAT that labels and enables the visualization of a broad spectrum of newly synthesized neuronal proteins *in situ* using conventional fluorescence microscopy. We name this visualization approach FUNCAT (FlUorescent Non–Canonical Amino acid Tagging).

Results

Fluorescent *in situ* tagging of newly synthesized proteins

Given limited current methods, we sought to develop a methodology for the *in situ* visualization of newly synthesized proteins using fluorescence microscopy. Building on the core chemistry of BONCAT, we synthesized two different fluorescent tags (TexasRed–PEO_2–Alkyne, TRA; 5'–carboxyfluorescein–PEO_8–Azide, FLA) that can be coupled to AHA– or HPG–bearing proteins using click chemistry23 (Fig. 1a,b; Supplementary Fig. 1). For the tag synthesis, the use of the water soluble linker polyethylene oxide (PEO) simplifies the synthesis, making it tractable in a biology laboratory setting18, and also maximizes the signal–to–noise ratio of the fluorescent labeling as any unligated tag is easily removed by washes.

We optimized the labeling and reaction conditions to maximize the specific detection of newly synthesized proteins *in situ* and to permit immunolabeling. To maximize charging and incorporation of the methionine surrogates AHA or HPG, we removed growth media from the preparations and replaced it with HBS or HibA media for 30 min prior addition of AHA or HPG. Following bath application of either AHA or HPG, we fixed and permeabilized neurons using Triton X–100. After overnight incubation in a reaction mixture that included the fluorescent tag, the copper catalyst and the triazole ligand, we visualized (Fig. 1b), newly synthesized proteins using conventional fluorescence microscopy. Incubation of primary hippocampal neurons with AHA or HPG for 1 h (in the absence of methionine) resulted in abundant labeling of newly synthesized proteins in somata and dendritic processes (Fig. 2a, first and third rows from top) at comparable levels for both AHA and HPG. Importantly, when protein synthesis was prevented by co–application of the protein synthesis inhibitor anisomycin, the fluorescent signal was dramatically reduced (Fig. 2a, second and fourth rows from top) confirming that this procedure labeled newly synthesized proteins with high specificity. Moreover, to further test the specificity of the approach we either omitted the copper catalyst in the click reaction mixture or co–applied methionine at an equimolar concentration, which prevented detection or incorporation, respectively, of AHA and HPG–derived signals (Supplementary Fig. 2). Following the click reaction, neurons can also be processed for conventional immunocytochemistry; we demonstrated this by immunolabeling with the dendritic marker MAP2 in AHA– or HPG–treated neurons (Fig. 2a). The combination of FUNCAT with immunolabeling did not alter the FLA or TRA signal intensity or result in crosstalk of the red and green image acquisition channels.

Following a 1 h incubation with either AHA or HPG, newly synthesized proteins were detected in both the somata and dendrites. Longer (∼2 h) exposures to AHA or HPG revealed the presence of newly synthesized proteins in spine–like protrusions from dendrites (Fig. 2b). This signal likely represents the presence of newly synthesized proteins at synapses as evidenced by proximity to the presynaptic protein Bassoon. Notably, we did not detect any changes in neuronal morphology in somata or dendrites, nor elevated levels of cell death, indicating no apparent toxicity resulting from AHA and HPG incubation for any concentration or methionine starvation period tested (see also ref.22). Taken together, these

data indicate that non–canonical amino acids coupled to fluorescent tags via click chemical reactions can be used to visualize newly synthesized proteins with high specificity.

We next examined if visualization of newly synthesized proteins can be performed in intact tissue using organotypic hippocampal slices. We increased the duration of exposure to AHA (to 4 h) to allow penetration of the amino acid into the depth of the slice (ca. 150 μm thick). As demonstrated in Supplementary Fig. 3, AHA–tagged proteins are present in somata and dendrites throughout the entire slice following labeling with AHA for 4 h. Application of the protein synthesis inhibitor anisomycin (40 μM) together with AHA completely blocked the fluorescent signal, indicating that protein synthesis is required for the fluorescence visualization. In Supplementary Fig. 3, the combination of FUNCAT with immunolabeling for MAP2 showed that newly synthesized proteins detected in organotypic slices are present in both the cell bodies and the dendrites of hippocampal neurons. The remaining FUNCAT signal that is not accounted for by the somatic and dendritic label likely is due to new protein synthesis in axons and glia based on immunostaining experiments using the axonal marker Tau (Supplementary Fig. 4) and the astroglial marker GFAP in dissociated cortical cultures (DC Dieterich, unpublished observations).

In order to examine the effects of a particular treatment on a proteome, it is often desirable to conduct pulse–chase type experiments in which two different time intervals can be examined. As there are currently two different non–canonical amino acids available, we investigated the feasibility of sequential application of AHA and HPG, followed by a click reaction with their complementary fluorescent TRA and FLA tags. There were two major considerations to adapt the technique for two intervals of labeling: first, optimization of the loading and incorporation of both AHA and HPG and second, optimization of the tag brightness, taking into consideration bleaching and the extended period of time from labeling to imaging. We tested all possible sequences of labeling (first AHA then HPG, or first HPG then AHA) and detection (TRA or FLA tag). For example, neurons were treated with HPG for 1 h and then washed and treated with AHA for 1 h. Following AHA treatment, neurons were fixed and exposed first to the FLA tag (overnight), followed by thorough rinses with PBS containing no EDTA to remove unligated tag, and then to the TRA tag (again, overnight) (or vice versa). This resulted in the fluorescent labeling of two distinct proteomes, synthesized in sequential time periods (Fig. 3) that was completely abolished if anisomycin was present during the application of AHA and HPG (data not shown). We analyzed the TRA and FLA signals in both the somatic and dendritic compartments and compared the label intensities for the different labeling orders. We found that application of HPG prior to labeling with AHA yielded the brightest and most consistent labeling (see also Supplementary Fig. 5); this fits with *in vitro* observations that charging of HPG onto methionyl tRNA is slower than charging of AHA16. Therefore, by using HPG in the first pulse followed by the AHA pulse the slower charging rate can be neglected. In addition, we determined that ligation of the TRA tag prior to the FLA tag is preferable, most likely since the TexasRed dye is less prone to photo degradation and bleaching than the fluorescein fluorophore24, a fact that might be overcome by using fluorophores with the same stability features. Thus, the optimal sequential tagging strategy for labeling two intervals of protein synthesis is HPG then AHA then TRA then FLA. This approach, coupled with a period of

stimulation, should provide an informative means to visualize changes in neuronal protein synthesis.

Sensitivity of FUNCAT

To investigate how quickly newly synthesized proteins can be visualized, we performed a time–course experiment, varying the duration of exposure to either AHA or HPG. To capture early events of translation we imaged neurons with high resolution after FUNCAT and MAP2 immunostaining. We analyzed the signal intensities of newly synthesized proteins of straightened dendrites using the MAP2–defined area as a mask. Strikingly, newly synthesized proteins can be detected in neuronal somata following a brief 10 min AHA or HPG exposure (Fig. 4a,b; Supplementary Fig. 6, respectively). Increasing the duration of AHA or HPG exposure resulted in a more intense fluorescent signal in cell bodies and the emergence of signal in the dendrites. Newly synthesized proteins in proximal dendrites were visible as early as 20 min after incubation (Fig. 4c,d), with signals increasing in intensity and expanding into distal dendritic segments within 2 h. We compared the relative efficacy of AHA and HPG and found no difference in tagging performance for AHA or HPG for time points over 30 min. However, for early time points (10 min and 20 min) AHA appears to be incorporated faster into nascent proteins compared to HPG, again consistent with previously published charging rates of AHA and HPG by the methionyl–tRNA synthetase (MetRS)16.

Monitoring BDNF–Induced Proteome Dynamics with FUNCAT

Protein translation enables neurons to respond rapidly to changes in the environment or activity pattern. BDNF (brain–derived neurotrophic factor) is an important modulator of neuronal activity during development as well as in the adult organism, and has been implicated in regulating neuronal survival, signaling and activity–dependent synaptic plasticity25. Moreover, it has been shown that BDNF elicits a protein synthesis dependent enhancement of synaptic strength12,26. In addition, BDNF induced an increase in dendritic translation of a GFP–based reporter construct in mechanically and optically isolated dendrites12. To examine the effects of synaptic stimulation on protein translation and on the localization of newly synthesized proteins, we performed bath application experiments with BDNF in the presence of AHA, followed by detection of AHA–harboring proteins with FUNCAT. In these experiments, we detected a 1.6–fold increase in the signal of newly synthesized proteins in proximal segments of BDNF–treated dendrites over controls (vehicle) after bath application of BDNF (50 ng/ml) for 1 h (Fig. 5a,b). In these experiments, the distal dendrites showed a less BDNF–induced increase in translation that may be attributed to the low signal–to–noise ratio associated with fluorescence imaging in tiny processes. These data demonstrate that FUNCAT can be used to visualize changes in protein synthesis in intact neurons.

Exploring the site of translation

The above experiments, in which AHA or HPG was introduced in the bath, do not address the site (somata or dendrites) of protein synthesis. To examine dendritic protein synthesis in a context where somatic synthesis is minimized, we locally perfused a protein synthesis inhibitor over a neuronal cell body while AHA was applied to the bath. To examine whether

the non–canonical amino acids can be taken up across dendritic membranes and locally incorporated into proteins, we examined the localization of the amino acid transporter LAT1 and MetRS. Both proteins were detected in the somata and dendrites, exhibiting a punctate distribution pattern (Supplementary Fig. 7). Using small delivery and suction pipettes, we microperfused anisomycin over the soma while AHA was bath–applied in the presence or absence of BDNF (Fig. 6a). 30 min after addition of AHA (or AHA + BDNF) to the bath, we fixed and processed cells for FUNCAT staining and MAP2 immunostaining. As previously observed, BDNF enhanced the new protein synthesis signal in both the cell bodies and the dendrites (Fig. 6b,c). We then addressed the contribution of somatic protein synthesis to this enhancement by introducing the perfusion of anisomycin over cell bodies. The somatic perfusion of anisomycin diminished the signal intensity of newly synthesized proteins in the soma to levels comparable to that observed when anisomycin and AHA were bath applied (Fig. 6b). These data suggest that the local perfusion of anisomycin is as effective as bath application in inhibiting protein synthesis. Interestingly, the distal segments of dendrites from neurons perfused at the soma with anisomycin exhibited AHA–derived intensity levels that were comparable to dendrites from nonperfused neurons (compare green bars in Fig. 6c to purple bars in Fig. 6d), suggesting a dendritic synthesis source for this AHA–derived signal. Moreover, as observed previously (e.g. Fig. 5), the addition of BDNF resulted in an increase of translation over the entire dendrite. Statistical analysis (one–way ANOVA with post–hoc Tukey multiple comparison testing) revealed a significant main effect both of treatment and dendritic segment; the interaction was also significant ($p = 0.0125$ for the first proximal 100 μm, and $p = 0.0473$ for the second 100 μm).

To examine directly whether non–canonical amino acids can be locally incorporated into proteins synthesized in dendrites, we selectively microperfused AHA onto single distal dendrites (Fig. 7a). In these experiments, we combined local dendritic microperfusions with bath application of anisomycin to reduce the likelihood of 2 events: i) AHA incorporation into proteins at sites adjacent to the dendritic perfusion area (due to possible intracellular diffusion of AHA; Fig. 7b) and ii) retrograde transport of AHA to the soma followed by incorporation of AHA into somatically synthesized proteins. When compared to nonperfused dendrites (Fig. 7b,c), the local perfusion of AHA led to detectable *de novo* protein synthesis in dendrites, inside as well as outside of the perfused area. Signal for newly synthesized proteins, however, was more prominent within the perfused area with a slight gradient of intensity towards the soma. The latter observation might be explained by retrograde transport of AHA–labeled proteins to the soma (synapse to nucleus communication) as well as the geometrical properties of the dendrite itself. As predicted, co–perfusion of AHA and BDNF (50 ng/ml) resulted in an increase in dendritic translation (ranging from 1.2 – 1.7 fold). Moreover, newly synthesized proteins were found to a larger extent in regions adjacent to the perfused area, indicating that local application of the neurotrophin also may affect the translation in or diffusion to neighboring synaptic regions. To exclude the possibility that local microperfusion itself exerts these effects, we repeated the last experiment in combination with AHA bath application (Supplementary Fig. 8). Here, microperfusion of AHA results in negligible changes in protein translation, whereas local co–application of BDNF produced a pronounced increase in *de novo* protein synthesis.

Diffusion properties of new proteins at neuronal membranes

In the previous experiments, the copper–dependent click reaction that couples the newly synthesized proteins to our fluorescent tags required fixation of the sample. We next analyzed the mobility of individual newly synthesized proteins in the membrane of living neurons, using Single Particle Tracking (SPT) experiments in which Quantum dots (QDs) were coupled to membrane proteins tagged with AHA (Fig. 8a). Given their brightness and photostability, QD nanoparticles are powerful fluorescent probes for SPT27. After a brief (∼ 30 min) methionine deprivation, neurons were incubated with AHA, Met or AHA + anisomycin for 2–4 hours to allow new proteins to be synthesized and trafficked to the cell surface. The detection of AHA–labeled proteins in living cells involved the use of a copper–free click chemistry method28, based on the covalent coupling of the azide group of AHA–tagged proteins with an alkyne–bearing reagent, a difluorinated cyclooctyne (DIFO), a membrane impermeant reagent. Subsequently, neurons were incubated in DIFO–biotin derivative, washed, and labeled with streptavidin–conjugated Quantum Dots (QD–SA) for 1 min.

As shown in Fig. 8b, QD labeling in living and non–permeabilized cells resulted in newly synthesized AHA–containing, QD–associated proteins detected both on neurites and somata. The QD–labeling was specific as a very few QD were associated with the neuronal surface in control conditions (Fig. 8b).

We characterized the motions of QD–labeled proteins (Fig. 8c) after trajectory reconstruction, and determined their relationship to synapses with FM4–64 staining (Fig. 8c). The high signal–to–noise ratio of QDs enables one to estimate their position with an accuracy of 10–20 nm29. The plot of the mean square displacement (MSD) as a function of time indicates the type of movement: at the extrasynaptic membrane, newly synthesized proteins had a Brownian–like behavior as indicated by the almost linear MSD vs time plot; at synapses, the movement was confined since the plot tended toward an asymptote (Fig. 8d). The cumulative distribution of diffusion coefficients (D) of newly synthesized proteins emphasized the heterogeneity of diffusive behaviors. D values spread over 5 orders of magnitude (10^{-4} <D< 1 $\mu m^2/s$) with a bimodal distribution (Fig. 8e,f), likely reflecting the diversity of synthesized proteins. At extrasynaptic regions, a fast moving population ($2{,}5.10^{-2}$ <D<1 $\mu m^2/s$) represented 50% of the trajectories, and a slow one (D<$10^{-3}\mu m^2/s$) represented 35% of the trajectories. AHA–tagged proteins were slower at synapses than outside synapses, with a similar number of immobile QDs (65% and 50%, respectively). We compared the D distribution of the population of newly synthesized proteins to that of defined membrane proteins, such as the γ2–$GABA_A$ receptor subunit in hippocampal neurons at 15 DIV (Fig. 8e,g). Interestingly γ2–$GABA_A$ receptor had a unimodal distribution of D with 75% of values between 6.10^{-3} and 6.10^{-2} $\mu m^2/s$ (G Gouzer, personal communication), spanning only a sub–range of that of the whole pool of newly synthesized proteins. This was also the case for the GFP–GPI30, the mGluR531,32 or the AMPAR (GluR2[33]). Interestingly, each individual protein had a specific pattern of mobility, which is reflected in the distribution of the diffusion coefficients; the diffusion coefficient of the newly synthesized proteins, in contrast, spans over the distribution of any individual protein

(Fig. 8f). Other parameters such as confinement and dwell time in given compartments were distinct as well (data not shown).

DISCUSSION

Synapses possess a complex mixture of proteins including receptors, regulatory and scaffolding proteins. Despite a clear need, dynamic visualization of the complete dendritic and/or synaptic proteome is still lacking. Indeed, new protein synthesis during synaptic plasticity is often inferred from electrophysiological recordings, rather than directly visualized or detected4,6,26,34,35. In a few cases, however, the direct visualization of a single type of newly synthesized protein has been achieved with great effort12,14,36,37. Owing to the techniques used (fluorescent reporters or antibodies) these studies have necessarily focused on one or two candidate proteins at a time.

Bioorthogonal chemistry provides an alternative to these methods as it lends novel functionality to endogenous proteins using chemical groups that are not readily found in living organisms. We demonstrate that a brief (∼10 min) application of either AHA or HPG followed by a click reaction with a fluorescent (azide– or alkyne–bearing) tag gives rise to a clearly detectable signal in neuronal somata. A slightly longer (∼20 min) exposure to AHA or HPG allows one to visualize newly synthesized proteins in dendrites. To visualize newly synthesized proteins we developed two fluorescent alkyne probes, TRA and FLA, for ligation to AHA– or HPG–labeled proteins. A previous study used HPG together with a 3–azido–7–hydroxycoumarin tag to visualize newly synthesized proteins in heterologous cells38. The TRA and FLA tags are better for tagging newly synthesized proteins in dissociated neuronal cultures and organotypic slices compared to the coumarin dye, because there is less background labeling associated with the tag sticking to the poly–D–lysine coating of the dishes used for culturing dissociated neurons. The synthesis can be easily adapted to develop similar PEO–linker featured fluorescent tags using different fluorophores to accommodate special needs such as STED high–resolution microscopy. Importantly, the recent development of alkyne-tags that can be coupled to azides via strain–promoted cycloaddition39 enabled us to examine the spatial dynamics of *de novo* synthesized membrane proteins in real time.

The specific compartment where proteins are synthesized is important for understanding both the cell biology and the logic of synaptic function and plasticity. Using microperfusion techniques to effect the selective exposure of somata or dendrites to AHA and/or a protein synthesis inhibitor we observed the spatial origin of the newly synthesized proteins in both cell bodies and dendrites. In future studies this technique can be used to visualize the trafficking and destination of proteins synthesized in distinct neuronal compartments. Here, the use of microfluidic cell culture devices40 to accommodate the spatially restricted delivery of metabolites and reagents may allow one to investigate the contributions of somatic and dendritic protein synthesis to synaptic plasticity. For example, there is considerable interest in the idea of “synaptic tagging” where synaptic signals stimulate transcription and/or translation in the soma and the mRNAs or proteins generated are “captured” at those synapses that have been tagged. Thus far, the capture of new proteins has been inferred by clever electrophysiological and pharmacological manipulations4,6,41–

43. The techniques described here would allow one to directly visualize the capture phenomenon.

Since the technique works both in dissociated neurons and in brain slices, labeling *in vivo* may also be possible. In this case, the ability to label sub–populations of neurons has distinct advantages for both visualization and circuit analysis. We have recently described a new system that may permit such visualization44. In this system, a mutant version of the MetRS is introduced which incorporates a modified non–canonical amino acid (azidonorleucine; ANL) into protein. Cell or promoter–specific labeling can be effected by the selective expression of the mutant MetRS in a particular cell population; ANL is not charged by the endogenous MetRS and as such will only label proteins in the identified cell population.

The earliest demonstrations that new protein synthesis is important for long–term memory were behavioral studies in both rodents45 and fish46. Using modifications of the techniques we describe above, we should be able to visualize, directly, protein synthesis in neural circuits involved in learning and memory.

Methods

Reagents

We purchased all reagents at ACS grade from Sigma unless noted otherwise. We purchased brain–derived neurotrophic factor (BDNF) from Promega, and used it at a concentration of 50 μg/ml. We purchased HPG from Chiralix (The Netherlands).

Organic Synthesis

We prepared AHA and the triazole ligand as described previously47. We prepared the TexasRed–PEO_2–Alkyne by dissolving TexasRed–PEO_2–propionic acid succinimidyl ester (Biotium Inc.) in excess neat propargylamine (Sigma–Aldrich). After 30 min, we added the solution dropwise to anhydrous diethyl ether. We collected the resulting precipitate by centrifugation (5 min, 10°C, 10.000 × g). Then, we washed the precipitate three times with anhydrous diethyl ether, dried and characterized it by ion spray MS to confirm the formation of the product with a molecular weight of 802.90 g/mol (Supplementary Fig. 1a). We synthesized the azide–bearing fluorescein tag in a similar way using the amine–reactive 5–carboxyfluorescein–PEO_8–propionic acid succinimidyl ester (Biotium Inc.) and 3–azidopropan–1–amine20 to yield a product with a molecular weight of 881.20 g/mol (Supplementary Fig. 1b).

Cultured Hippocampal Neuron and Organotypic Hippocampal Cultures

We prepared and maintained dissociated hippocampal neurons as previously described12. Briefly, we dissected out and dissociated hippocampi from postnatal day 0 to 2 rat pups (strain Sprague–Dawley) by either trypsin or papain and plated at a density of 40,000 cells/cm^2 onto poly–D–lysine–coated glass–bottom Petri dishes (Mattek). We maintained these cultures in Neurobasal A medium containing B–27 and Glutamax supplements (Invitrogen) at 37°C for 18–24 days before use. We prepared organotypic hippocampal cultures according to Gogolla et al.48, and maintained in culture for three weeks before use.

Copper–Catalyzed [3+2]–Azide–Alkyne–Cycloaddition Chemistry (CuAAC) and Detection of Tagged Proteins

In all culture experiments, we removed the growth medium from neuronal cultures and replaced it with either HEPES–buffered solution (HBS)12 or methionine–free Hibernate A (HibA) medium (BrainBits LLC.) for 30 min to deplete endogenous methionine. We observed no difference in protein synthesis between neuronal cultures incubated in HBS or HibA for time points tested (up to 2 hours). However, we opted to use HibA after it became available as a defined and customizable minimal neuronal growth media to optimize and standardize our labeling procedure. For AHA labeling, we supplemented HBS and HibA with 2 mM AHA, 2 mM AHA plus 40 μM anisomycin, or 2 mM methionine. After incubation at 37°C, 5% CO_2, we washed cells with chilled PBS–MC (1mM $MgCl_2$, 0.1 mM $CaCl_2$ in PBS) on ice to remove excess amounts of AHA and methionine followed by immediate fixation with chilled 4% paraformaldehyde, 4% sucrose in PBS–MC for 20 min at room temperature (RT).

For CuAAC, in order to avoid copper bromide–derived precipitates, we used TCEP in combination with copper sulfate to generate the Cu(I) catalyst during the CuAAC reaction. Briefly, a CuAAC reaction mix composed of 200 μM triazole ligand (stock solution dissolved at 200 mM in DMSO), 2 μM fluorescent alkyne or azide tag, 400 μM TCEP and 200 μM $CuSO_4$ was mixed in PBS (pH 7.6) with vigorous vortexing after each addition of a reagent. We incubated hippocampal primary cultures or organotypic hippocampal slices overnight at 20°C with the CuAAc reaction mix in a humid box under gentle agitation. Following incubation, we washed cells or slices three times for 10 min each at RT with 1% Tween–20, 0.5 mM EDTA in 1x PBS pH 7.4 followed by three rinses with 1x PBS pH 7.4 prior to immunostaining using standard conditions. We tested AHA and HPG concentrations ranging from 0.1 mM to 4 mM and observed saturated labeling at a 2 mM concentration without any apparent toxicity or any change in gross cellular morphology (data not shown). Therefore, we used 2 mM AHA or HPG in all subsequent experiments.

For immunolabeling after AHA incorporation and cycloaddition, we treated primary cells sequentially with PBS, blocking solution (0.1% Triton X–100, 2 mg/ml BSA, 5% sucrose, 10% normal horse serum in PBS), primary Ab in blocking solution at 4°C overnight or at RT for 2 h, PBS–Tx (0.1% Triton X–100 in PBS), Alexa488– or Alexa568–conjugated secondary Ab (Invitrogen) in blocking solution, PBS–Tx and PBS, and mounted in Gold Prolonged Antifade reagent (Invitrogen) prior to imaging. For immunolabeling and cycloaddition of AHA–tagged proteins in organotypic cultures, we fixed slices overnight at 4°C, rinsed extensively several times, blocked and permeabilized overnight in blocking solution before performing CuAAC for at least 12 h at RT. We performed immunostaining for MAP2 as described above with extensive washes and prolonged incubation periods with secondary antibodies. We used the following primary antibodies: rabbit anti–microtubule–associated protein 2 (anti–MAP2) polyclonal (1:1000, Chemicon), mouse anti–MAP2 monoclonal antibody (Sigma, 1:500), mouse anti–bassoon monoclonal (1:1000, Stressgen Bioreagents Corp.), mouse anti–Tau (1:400, Chemicon), goat anti–LAT1 (L13) polyclonal antibody (Santa Cruz, 1:100), rabbit anti–methionyl tRNA synthetase polyclonal antibody

(abcam, 1:500). For secondary antibodies, we used anti–rabbit or anti–mouse conjugated Alexa Fluor 488, 568, or 647 (1:500; Invitrogen).

Local Perfusions

Local perfusion experiments were performed with an Olympus IX–70 confocal laser–scanning microscope using Plan–Apochromat 40x/0.95 air or 40x/1.0 oil objectives. We excited Alexa 488 with the 488 nm line of an argon ion laser, and collected the emitted light between 510 and 550 nm. For restricted treatment of isolated somata or dendritic segments, we used a dual micropipette local delivery system. The delivery micropipette was pulled as a typical whole–cell recording pipette with an aperture of ∼ 0.5 μm. We controlled the area of local perfusion by a suction pipette, using it to draw the treatment solution across one or more dendrites and to remove the perfusion solution from the bath. In all microperfusion experiments we monitored the dimension of the perfusion spot with the fluorescent dye Alexa Fluor 488 hydrazide (1 μg/ml, Invitrogen) throughout the duration of the experiment; perfusion spot diameters ranged from 30 to 50 μm). We used only the experiments in which the affected area changed by less than 20% for analysis. In all local perfusion experiments, we maintained the set–up at 32°C with a closed box–incubator around the microscope and used multiple small water pans to keep the system humid. We started somatic perfusions with anisomycin (40 μM) 20 min before bath application of 2 mM AHA or 2 mM AHA + BDNF (50ng/ml; 30 min incubation) to decrease somatic translation to minimal levels. After fixation, we performed FUNCAT using 1 mM TRA tag and immunostained for MAP2. We determined the size of the treated area for each soma or dendrite based on Alexa 488 fluorescence integrated across all images (typically 6–10) taken during local perfusion

Microscopy and image analysis

Unless otherwise specified, we acquired images with a Zeiss 510 Meta confocal laser scanning microscope. We excited Alexa 488 and 5–carboxyfluorescein with the 488 nm line of an argon ion laser, and collected the emitted light between 510 and 550 nm. We excited TexasRed with the 568 nm line of a krypton ion laser, and collected the emitted light above 600 nm. In experiments where two channels were acquired simultaneously, we chose settings to ensure no signal bleed–through between channels. For between–dish comparisons on a given day, we acquired all images using the same settings, without knowledge of the experimental condition during image acquisition. We performed all postacquisition processing and analysis with ImageJ (NIH) and Imaris (Bitplane Scientific Software). To facilitate the analysis of fluorescence signal as a function of distance from the soma, we linearized dendrites and extracted their unprocessed full–frame images using the Straighten plugin for ImageJ. For the analyses of local perfusion experiments, we calculated the TRA signal intensity per volume using a 3D–mask that was generated from the corresponding MAP2 stacks of straightened dendrites in 10 μm volume segments using Imaris.

Copper–free click chemistry and single particle imaging

We performed QD experiments on 8–12 DIV hippocampal neurons. First, we deprived cells of methionine for 30 min in HBS, and then incubated with HBS supplemented with 2 mM AHA, 2 mM AHA + 40 μM anysomycin, or 2 mM methionine for 2–4 hours at 37°C, 5% CO_2. For the click chemistry reaction, we washed and incubated cells in 1μM DIFO–

biotin29 for 5 minutes at room temperature (20–25°C). Following 5–10 washes, we then incubated coverslips for 1 min at 37°C with streptavidin–coated quantum–dots emitting at 605 nm (1 nM, Invitrogen) in borate buffer (50 mM) supplemented with sucrose (200 mM). We extensively (~5 times) rinsed cells in HBS and exposed them to KCl (40 mM) and FM4–64 (2 μM, Invitrogen) for 30 s to stimulate vesicle recycling at presynaptic sites. We then washed and imaged cells in an open chamber mounted on an inverted microscope (IX71, 60X objective, NA=1.45, Olympus). We detected QDs and FM4–64 using a Hg+ lamp and appropriate excitation and emission filters (QD: D455/70x, HQ605/20m, FM4–64: D535/50x, E590lpv2; Chroma Technology). We recorded QDs for 38.5 s at 13Hz (500 consecutive frames) with a CCD Camera (Cascade 512BFT, Roper Scientific) and Metaview (Meta Imaging). Average number of QD per movie in AHA, AHA+Anisomycin and Methionine conditions: 25, 3.5 and 6.2s; average number of mobile QDs: 8.3, 3.6, 0.8, respectively. For the analysis we did not take into account QDs with $D<10^{-4}$ $\mu m^2/s$. We performed $GABA_A$ receptor experiments on 15 DIV neurons immunolabeled with QDs as previously described 49.

Statistics

Results are presented as mean s.d./SEM for the indicated number of experiments. Statistical analyses were performed using one–way ANOVA and Student's *t*–test.

Supplementary Material

Refer to Web version on PubMed Central for supplementary material.

Acknowledgments

We thank L. Chen for making beautiful cultured hippocampal neurons. We thank A.J. Link for helpful discussions and help with the tag syntheses. We are grateful to O. Kobler for help with Imaris software. We are extremely grateful to both Carolyn Bertozzi and Jeremy Baskin for providing the difluorinated cyclooctyne–biotin and advise on its use. This work was supported by the German Academy for Natural Scientists Leopoldina (D.C.D.), the NIH (E.M.S. and D.A.T.), HHMI (E.M.S.) and the Ministère de l'Enseignement Superieur et de la Recherche (GG) and Nationale de la Recherche MorphoSynDiff–INSERM (A.T.).

References

1. Sutton MA, Schuman EM. Dendritic protein synthesis, synaptic plasticity, and memory. Cell. 2006; 127:49–58. [PubMed: 17018276]
2. Nguyen PV, Abel T, Kandel ER. Requirement of a critical period of transcription for induction of a late phase of LTP. Science. 1994; 265:1104–1107. [PubMed: 8066450]
3. Bito H, Deisseroth K, Tsien RW. CREB phosphorylation and dephosphorylation: a Ca(2+)- and stimulus duration-dependent switch for hippocampal gene expression. Cell. 1996; 87:1203–1214. [PubMed: 8980227]
4. Casadio A, et al. A transient, neuron-wide form of CREB-mediated long-term facilitation can be stabilized at specific synapses by local protein synthesis. Cell. 1999; 99:221–237. [PubMed: 10535740]
5. Kang H, Schuman EM. A requirement for local protein synthesis in neurotrophin-induced hippocampal synaptic plasticity. Science. 1996; 273:1402–1406. [PubMed: 8703078]
6. Martin KC, et al. Synapse-specific, long-term facilitation of aplysia sensory to motor synapses: a function for local protein synthesis in memory storage. Cell. 1997; 91:927–938. [PubMed: 9428516]

7. Weiler IJ, Wang X, Greenough WT. Synapse-activated protein synthesis as a possible mechanism of plastic neural change. Prog Brain Res. 1994; 100:189–194. [PubMed: 7938518]
8. Steward O. mRNA localization in neurons: a multipurpose mechanism? Neuron. 1997; 18:9–12. [PubMed: 9010200]
9. Liao L, et al. BDNF induces widespread changes in synaptic protein content and up–regulates components of the translation machinery: an analysis using high–throughput proteomics. J Proteome Res. 2007; 6:1059–1071. [PubMed: 17330943]
10. Manadas B, et al. BDNF-induced changes in the expression of the translation machinery in hippocampal neurons: protein levels and dendritic mRNA. J Proteome Res. 2009; 8:4536–4552. [PubMed: 19702335]
11. Takei N, et al. Brain-derived neurotrophic factor induces mammalian target of rapamycin-dependent local activation of translation machinery and protein synthesis in neuronal dendrites. J Neurosci. 2004; 24:9760–9769. [PubMed: 15525761]
12. Aakalu G, Smith WB, Nguyen N, Jiang C, Schuman EM. Dynamic visualization of local protein synthesis in hippocampal neurons. Neuron. 2001; 30:489–502. [PubMed: 11395009]
13. Macchi P, et al. A GFP-based system to uncouple mRNA transport from translation in a single living neuron. Mol Biol Cell. 2003; 14:1570–1582. [PubMed: 12686610]
14. Wang DO, et al. Synapse- and stimulus-specific local translation during long-term neuronal plasticity. Science. 2009; 324:1536–1540. [PubMed: 19443737]
15. Lin MZ, Glenn JS, Tsien RY. A drug-controllable tag for visualizing newly synthesized proteins in cells and whole animals. Proc Natl Acad Sci U S A. 2008; 105:7744–7749. [PubMed: 18511556]
16. Kiick KL, Saxon E, Tirrell DA, Bertozzi CR. Incorporation of azides into recombinant proteins for chemoselective modification by the Staudinger ligation. Proc Natl Acad Sci U S A. 2002; 99:19–24. [PubMed: 11752401]
17. Link AJ, Mock ML, Tirrell DA. Non-canonical amino acids in protein engineering. Curr Opin Biotechnol. 2003; 14:603–609. [PubMed: 14662389]
18. Link AJ, Tirrell DA. Cell Surface Labeling of Escherichia coli via Copper(I)-Catalyzed [3+2] Cycloaddition. J Am Chem Soc. 2003; 125:11164–11165. [PubMed: 16220915]
19. Zhang Z, et al. A new strategy for the site-specific modification of proteins in vivo. Biochemistry. 2003; 42:6735–6746. [PubMed: 12779328]
20. Beatty KE, Tirrell DA. Two-color labeling of temporally defined protein populations in mammalian cells. Bioorg Med Chem Lett. 2008; 18:5995–5999. [PubMed: 18774715]
21. Dieterich DC, et al. Labeling, detection and identification of newly synthesized proteomes with bioorthogonal non-canonical amino-acid tagging. Nat Protoc. 2007; 2:532–540. [PubMed: 17406607]
22. Dieterich DC, Link AJ, Graumann J, Tirrell DA, Schuman EM. Selective identification of newly synthesized proteins in mammalian cells using bioorthogonal noncanonical amino acid tagging (BONCAT). Proc Natl Acad Sci U S A. 2006; 103:9482–9487. [PubMed: 16769897]
23. Rostovtsev VV, Green LG, Fokin VV, Sharpless KB. A stepwise huisgen cycloaddition process: copper(I)-catalyzed regioselective "ligation" of azides and terminal alkynes. Angew Chem Int Ed Engl. 2002; 41:2596–2599. [PubMed: 12203546]
24. Whitaker JE, Haugland RP, Ryan D, Hewitt PC, Prendergast FG. Fluorescent rhodol derivatives: versatile, photostable labels and tracers. Anal Biochem. 1992; 207:267–279. [PubMed: 1481981]
25. Lewin GR, Barde YA. Physiology of the neurotrophins. Annu Rev Neurosci. 1996; 19:289–317. [PubMed: 8833445]
26. Kang H, Schuman EM. A requirement for local protein synthesis in neurotrophin-induced hippocampal synaptic plasticity. Science. 1996; 273:1402–1406. [PubMed: 8703078]
27. Alcor D, Gouzer G, Triller A. Single-particle tracking methods for the study of membrane receptors dynamics. Eur J Neurosci. 2009; 30:987–997. [PubMed: 19735284]
28. Baskin JM, et al. Copper-free click chemistry for dynamic in vivo imaging. Proc Natl Acad Sci U S A. 2007; 104:16793–16797. [PubMed: 17942682]
29. Dahan M, et al. Diffusion dynamics of glycine receptors revealed by single-quantum dot tracking. Science. 2003; 302:442–445. [PubMed: 14564008]

30. Renner M, Choquet D, Triller A. Control of the postsynaptic membrane viscosity. J Neurosci. 2009; 29:2926–2937. [PubMed: 19261888]
31. Serge A, Fourgeaud L, Hemar A, Choquet D. Receptor activation and homer differentially control the lateral mobility of metabotropic glutamate receptor 5 in the neuronal membrane. J Neurosci. 2002; 22:3910–3920. [PubMed: 12019310]
32. Renner M, et al. Deleterious effects of amyloid beta oligomers acting as an extracellular scaffold for mGluR5. Neuron. 2010 in press.
33. Renner ML, Cognet L, Lounis B, Triller A, Choquet D. The excitatory postsynaptic density is a size exclusion diffusion environment. Neuropharmacology. 2009; 56:30–36. [PubMed: 18694768]
34. Ouyang Y, Kantor D, Harris KM, Schuman EM, Kennedy MB. Visualization of the distribution of autophosphorylated calcium/calmodulin-dependent protein kinase II after tetanic stimulation in the CA1 area of the hippocampus. J Neurosci. 1997; 17:5416–5427. [PubMed: 9204925]
35. Waung MW, Pfeiffer BE, Nosyreva ED, Ronesi JA, Huber KM. Rapid translation of Arc/Arg3.1 selectively mediates mGluR-dependent LTD through persistent increases in AMPAR endocytosis rate. Neuron. 2008; 59:84–97. [PubMed: 18614031]
36. Ouyang Y, Rosenstein A, Kreiman G, Schuman EM, Kennedy MB. Tetanic stimulation leads to increased accumulation of Ca(2+)/calmodulin-dependent protein kinase II via dendritic protein synthesis in hippocampal neurons. J Neurosci. 1999; 19:7823–7833. [PubMed: 10479685]
37. Villareal G, Li Q, Cai D, Glanzman DL. The role of rapid, local, postsynaptic protein synthesis in learning-related synaptic facilitation in aplysia. Curr Biol. 2007; 17:2073–2080. [PubMed: 18006316]
38. Beatty KE, et al. Fluorescence visualization of newly synthesized proteins in mammalian cells. Angew Chem Int Ed Engl. 2006; 45:7364–7367. [PubMed: 17036290]
39. Agard NJ, Prescher JA, Bertozzi CR. A strain-promoted [3 + 2] azide-alkyne cycloaddition for covalent modification of biomolecules in living systems. J Am Chem Soc. 2004; 126:15046–15047. [PubMed: 15547999]
40. Taylor AM, et al. A microfluidic culture platform for CNS axonal injury, regeneration and transport. Nat Methods. 2005; 2:599–605. [PubMed: 16094385]
41. Frey U, Morris RG. Synaptic tagging and long-term potentiation. Nature. 1997; 385:533–536. [PubMed: 9020359]
42. Huang T, McDonough CB, Abel T. Compartmentalized PKA signaling events are required for synaptic tagging and capture during hippocampal late-phase long-term potentiation. Eur J Cell Biol. 2006; 85:635–642. [PubMed: 16600423]
43. Sajikumar S, Navakkode S, Frey JU. Identification of compartment- and process-specific molecules required for "synaptic tagging" during long-term potentiation and long-term depression in hippocampal CA1. J Neurosci. 2007; 27:5068–5080. [PubMed: 17494693]
44. Ngo JT, et al. Cell-selective metabolic labeling of proteins. Nat Chem Biol. 2009; 5:715–717. [PubMed: 19668194]
45. Flexner JB, Flexner LB, Stellar E. Memory in mice as affected by intracerebral puromycin. Science. 1963; 141:57–59. [PubMed: 13945541]
46. Agranoff BW, Klinger PD. Puromycin Effect on Memory Fixation in the Goldfish. Science. 1964; 146:952–953. [PubMed: 14199725]
47. Wang Q, et al. Bioconjugation by copper(I)-catalyzed azide-alkyne [3 + 2] cycloaddition. J Am Chem Soc. 2003; 125:3192–3193. [PubMed: 12630856]
48. Gogolla N, Galimberti I, DePaola V, Caroni P. Long-term live imaging of neuronal circuits in organotypic hippocampal slice cultures. Nat Protoc. 2006; 1:1223–1226. [PubMed: 17406405]
49. Bannai H, Levi S, Schweizer C, Dahan M, Triller A. Imaging the lateral diffusion of membrane molecules with quantum dots. Nat Protoc. 2006; 1:2628–2634. [PubMed: 17406518]
50. Renner M, Specht CG, Triller A. Molecular dynamics of postsynaptic receptors and scaffold proteins. Curr Opin Neurobiol. 2008; 18:532–540. [PubMed: 18832033]

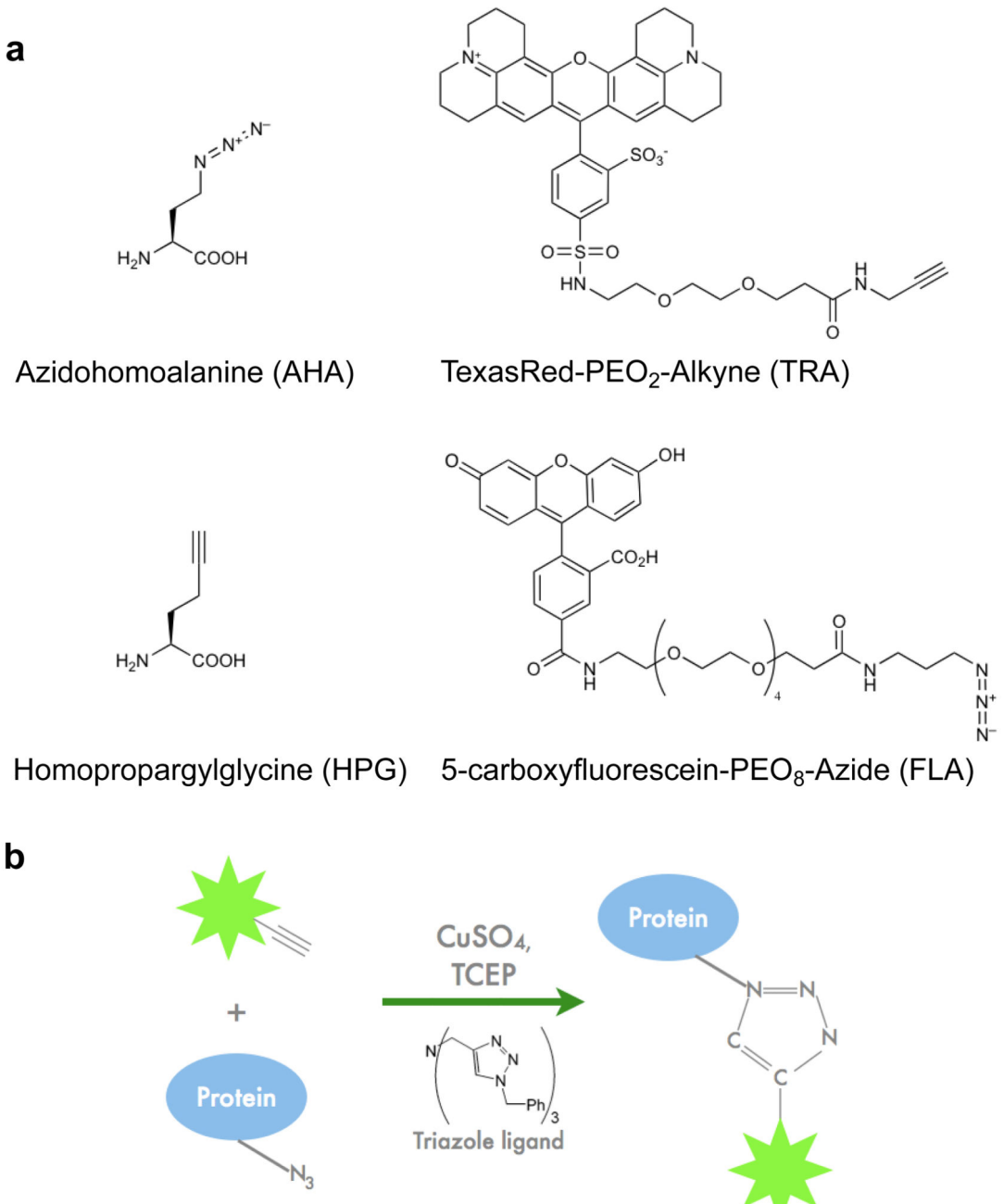

Figure 1. Chemical components and FUNCAT procedure

(**a**) Chemical structures of the modified amino acids azidohomoalanine (AHA) and homopropargylglycine (HPG), and the two fluorescent tags TexasRed–PEO2–Alkyne (TRA) and 5–carboxyfluorescein–PEO8–Azide (FLA) used in this study to visualize newly synthesized proteins. (**b**) Cartoon illustrating the Cu(I)–catalyzed [3+2] azide–alkyne cycloaddition (CuAAC) principle.

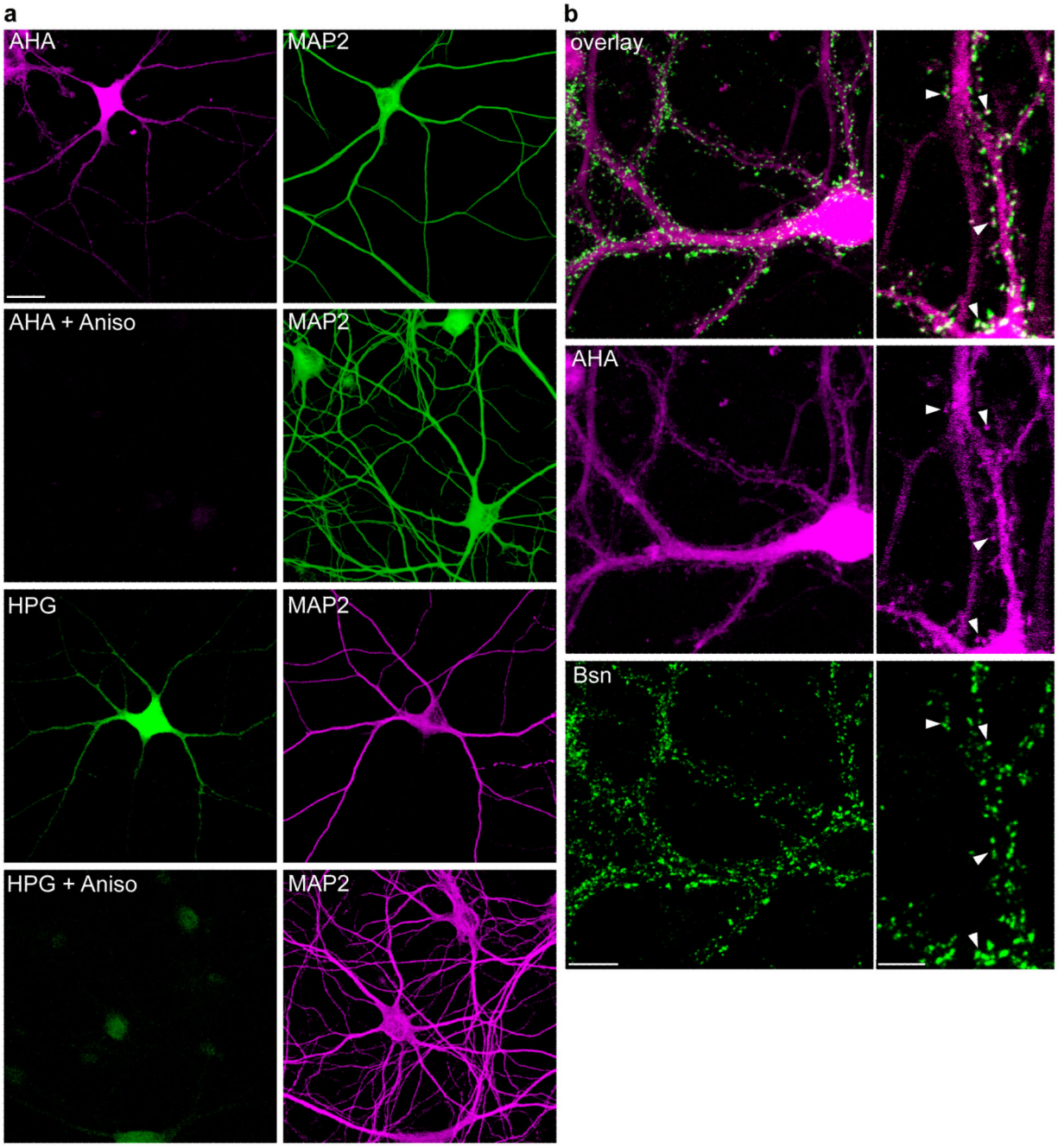

Figure 2. Visualization of newly synthesized proteins in dissociated primary hippocampal neurons

(**a**) Dissociated hippocampal neurons (DIV 17) were incubated with either 2 mM AHA or 2 mM HPG in the presence or absence of 40 μM anisomycin (Aniso) for 1 h, tagged with 1 mM TRA or FLA tag and immunostained for the dendritic marker protein MAP2. Scalebar = 20 μm. (**b**) Dissociated neurons were incubated with 2 mM AHA for 2 h followed by tagging with 1 mM TRA tag and immunostaining for Bassoon as a synaptic marker.

Arrowheads denote spine–like protrusions. Scalebar = 10 μm in the left panel images, scalebar = 5 μm in the magnified images.

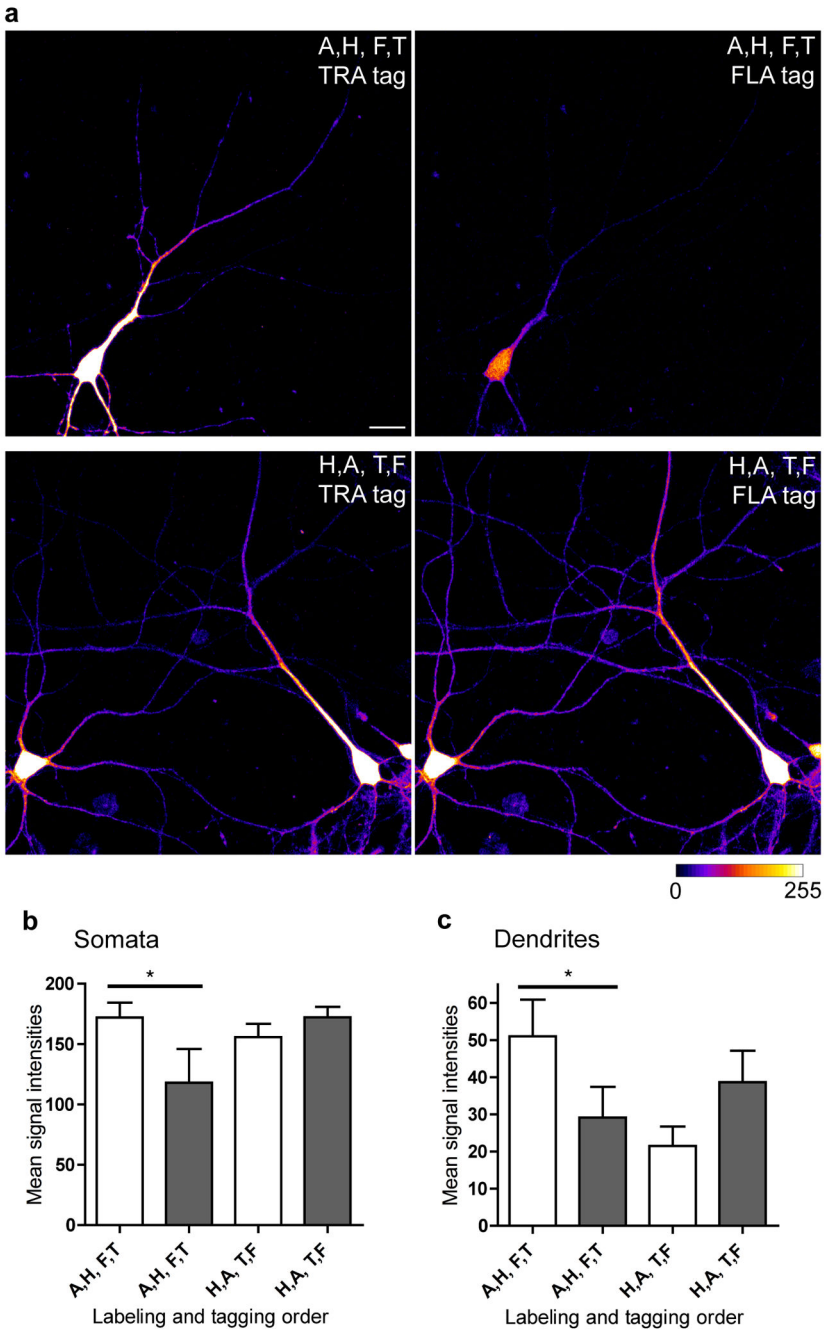

Figure 3. Sequential labeling of 2 newly synthesized protein pools with two metabolic markers

(**a**) Dissociated hippocampal neurons (DIV 16–18) were incubated in 2 mM AHA for 1.5 h followed by 4 mM HPG for 1.5 h and vice versa, and sequentially tagged with either 1 mM TRA then 1 mM FLA tag, or FLA tag followed by TRA tag for 12 hours each. Scalebar = 20 μm. Color lookup table indicates fluorescence intensity (pixel intensities 0–255). Labeling and detection sequences: A,H, F,T: first AHA then HPG, first FLA then TRA tag; H,A, T,F: first HPG then AHA, first TRA then FLA tag. Images were acquired and analyzed using identical parameters on a Zeiss Meta 510 confocal microscope using a 40x objective,

postprocessing and analysis was done with ImageJ. Graph (**b**) represents mean intensities ± SEM of somata for the indicated labeling and detection sequences. Graph (**c**) represents mean intensities ± SEM of dendrites (0–100 μm) for the indicated tagging and detection sequences. White boxes correspond to TRA signals, grey boxes indicate FLA signals. n = 6–10 neurons. P–values: ** $p < 0.005$; * $p < 0.05$.

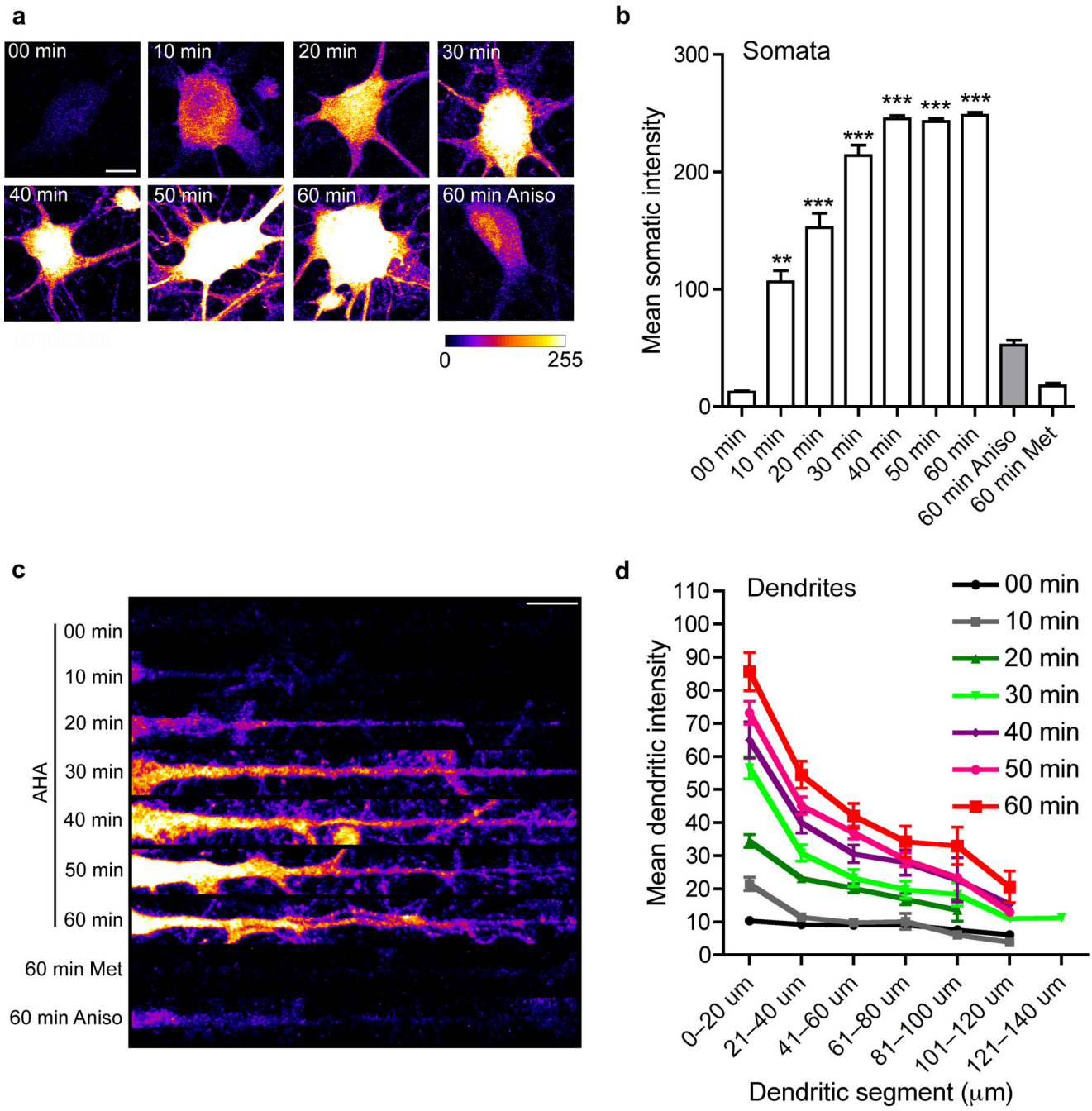

Figure 4. Time–course for the detection of newly synthesized proteins in somata and dendrites

(**a**) Cultures (DIV 16) were incubated for the time points indicated with 2 mM AHA, 2 mM methionine (Met) or 2 mM AHA in the presence of 40 μM anisomycin (Aniso). After cycloaddition with the fluorescent TRA tag, images were acquired with identical parameters on a Zeiss Meta 510 confocal microscope using a 63x objective. Scalebar = 5 μm. Graph (**b**) represents mean intensities ± SEM of the somata. Per time point, data from 20–50 cells were collected and analyzed using ImageJ. Representative examples are shown in the right panel. (**c**) Representative straightened dendrites of neurons incubated with 2 mM AHA, 2 mM

Methionine (Met) or AHA plus 40 μM anisomycin (Aniso) for time points indicated. Color lookup table indicates fluorescence intensity (pixel intensities 0–255). Left: proximal; right: distal. Scalebar = 10 μm. Graph (**d**) represents mean intensities ± SEM of the dendrites in 20 μm bins. Per time point data from 25–40 dendrites were analyzed. Note, that somatic signals are saturated in some cases, in order to optimize the imaging parameters for signal detection in distal dendrite segments.

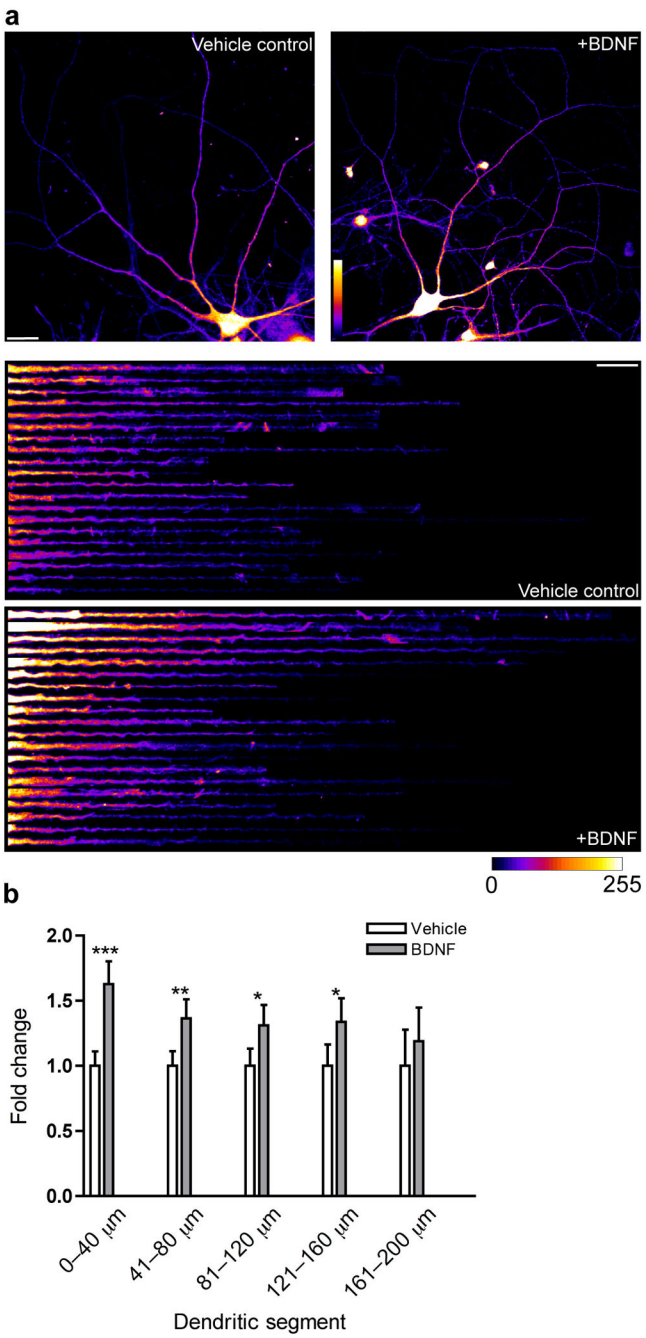

Figure 5. BDNF–induced increases in protein synthesis

(**a**) Hippocampal neurons (DIV 16) were incubated for 1 h with 2 mM AHA alone (vehicle control) or 2 mM AHA in the presence of 50 ng/ml BDNF. After a 15 min chase with 2 mM methionine, cells were fixed, tagged with 1 mM fluorescent tag and immunostained for the dendritic marker protein MAP2. For quantitative analysis, dendrites of both groups were straightened and fluorescent intensities of binned 40 µm segments were measured using ImageJ. Representative images for both groups are shown. Color lookup table indicates fluorescence intensity (pixel intensities 0–255). Note the increase in signal intensity in both

cell body and dendrites in BDNF–treated versus control cells. Left: proximal; right: distal. Scalebar = 20 μm. (**b**) Graph shows the change of TRA–signal of BDNF–treated cells ± SEM normalized to controls (vehicle). P–values: *** $p < 0.000005$; ** $p < 0.005$; * $p < 0.05$.

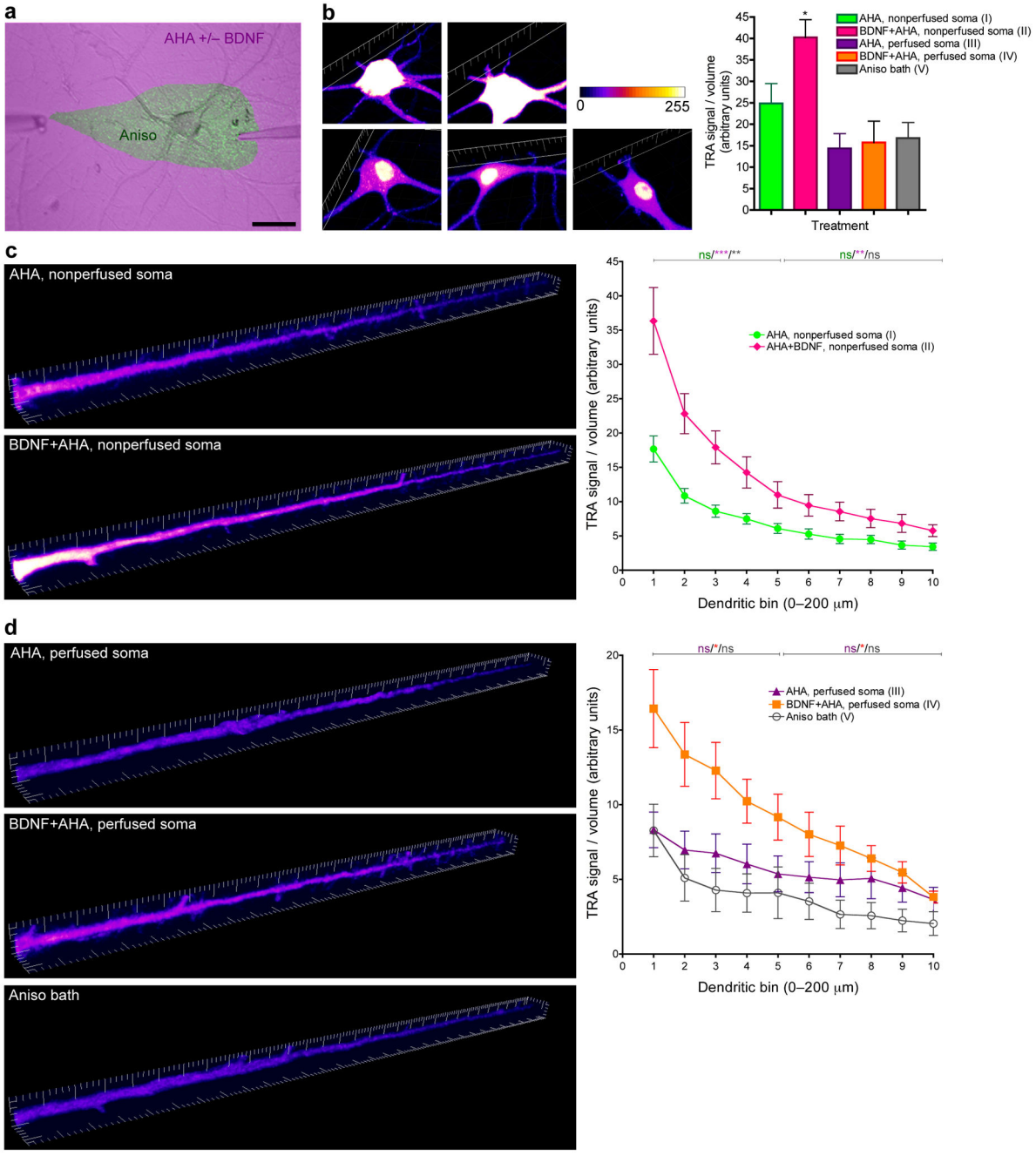

Figure 6. BDNF–induced increase in dendritic protein synthesis

(**a**) Somata of neurons were perfused with 40µM anisomycin before and during bath-application of 2 mM AHA, or 2 mM AHA + BDNF (50 ng/ml) for 30 min, scalebar = 50 µm. (**b**) Images showing signals of newly synthesized proteins from nonperfused somata (top left, AHA (I); top right, AHA + BDNF (II)), anisomycin–perfused somata (bottom left, AHA (III); bottom center, AHA + BDNF (IV)) and anisomycin–bath cells (bottom right, (V)). n = 6–9 cells. Large grid tick marks = 20 µm. Graph shows TRA–signal to volume ratios ± SEM. (**c,d**) Analysis of newly synthesized proteins in dendrites of groups I–IV.

Images show signal intensity of representative dendrites beginning at the soma. Left, proximal; right, distal. Color lookup table indicates fluorescence intensity. Note, that somatic signals are saturated in some cases, in order to optimize the imaging parameters for signal detection in distal dendrite segments. Large grid tick marks = 10 μm. Summary graphs shows signal to volume ratios ± SEM. n= 6–9 dendrites. P–values: *** $p < 0.001$; ** $p < 0.01$; * $p < 0.05$, one–way ANOVA with Tukey testing. In graph (**c**) significance values for group (I) vs. (V) dendrites are indicated in green, for group (II) vs. (V) in magenta, for group (I) vs. (II) dendrites in grey; in graph (**d**) significance values for group (III) vs. (V) dendrites are indicated in violet, for group (IV) vs. (V) in red, for group (III) vs. (IV) in grey.

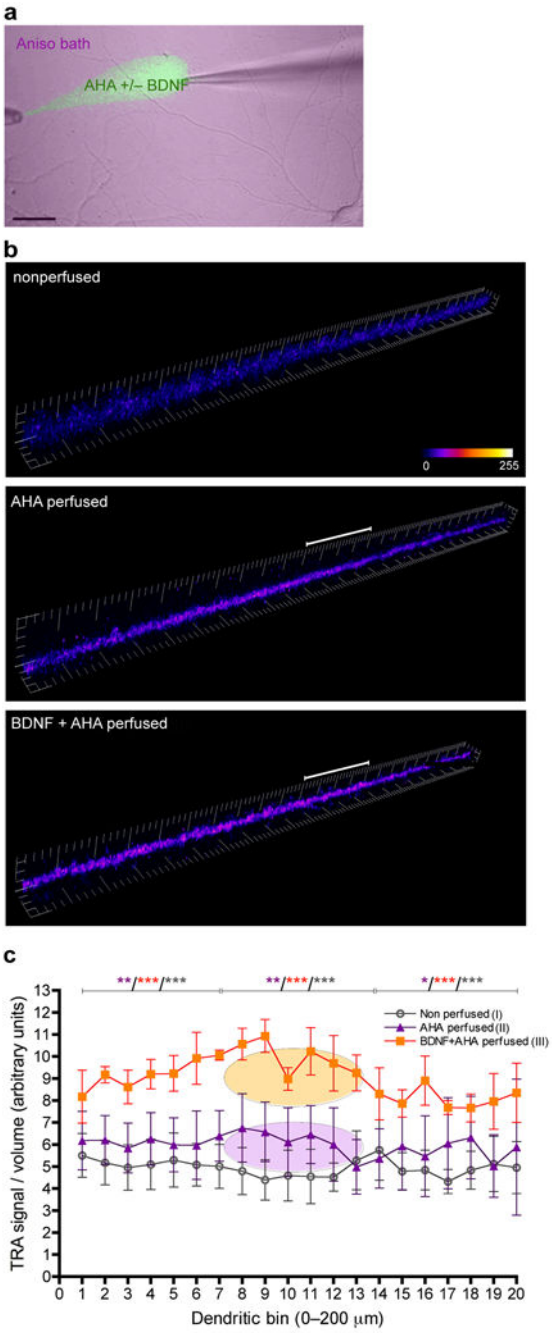

Figure 7. Local BDNF–induced increase in dendritic protein synthesis

(**a**) Hippocampal neurons for dendritic local perfusions in combination with anisomycin bath application were pre–incubated in 40 µM anisomycin for 20 min during which time the micropipettes were positioned. Dendritic local perfusion with 2 mM AHA in the presence or absence of BDNF (50 ng/ml) in HibA (with no anisomycin in the perfusion pipette) was initiated, and constantly monitored over the perfusion period of 30 min. Scalebar = 50 µm. Images (**b**) show TRA signals of representative dendrites from groups (I, top) no perfusion, (II, center) AHA perfusion, (III, bottom) BDNF plus AHA perfusion. Grey bars mark the

location and extension of the perfusion stream. Large grid tick marks = 10 μm. Color lookup table indicates fluorescence intensity. Graph (**c**) shows TRA–signal to volume ratios ± SEM. Colored ovals represent the positions of the perfusion spots. n= 4–5 dendrites. P–values: *** $p < 0.001$; ** $p < 0.01$; * $p < 0.05$ using one–way ANOVA statistical analysis with Tukey testing. Significance values are indicated for the dendritic segments before, within and beyond the perfusion spots; violet labels indicate significances for dendrites derived from group (I) vs. (II), red labels indicate significance values for group (I) vs. (III) dendrites, grey labels indicate significances for group (II) vs. (III) dendrites.

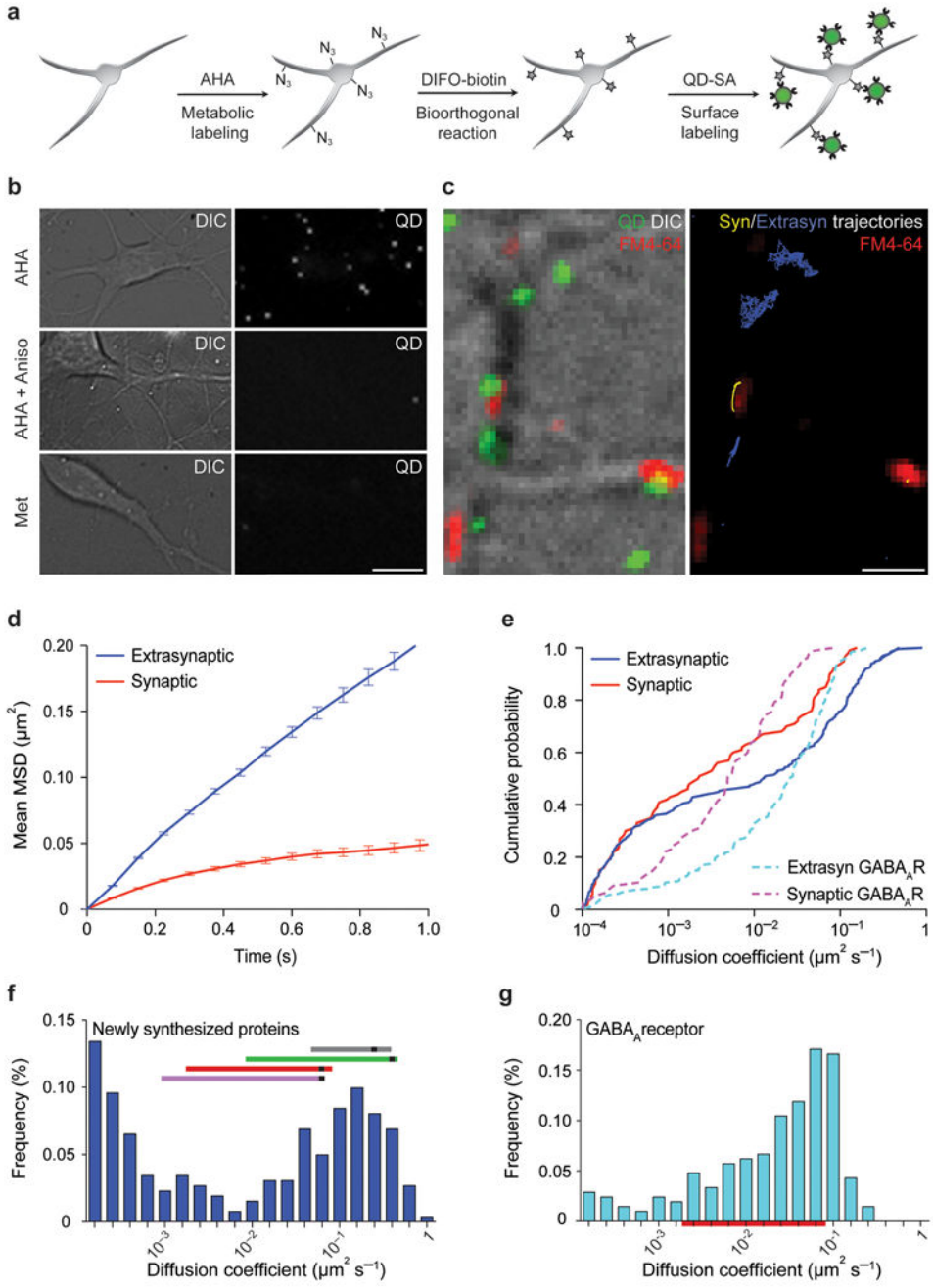

Figure 8. Diffusion properties of newly synthesized proteins at the surface of dissociated primary hippocampal neurons

(**a**) Strategy for labeling newly synthesized proteins inserted in the membrane of living neurons. (**b**) Neurons were incubated with either 2mM AHA in the presence or the absence of anisomycin, or 2mM Methionine for 2–4 hours and labeled with DIFO–biotin and QD–SA. DIC (left) and QD labeling (right) of live neurons from each condition. Scalebar = 5μm. (**c**) Example of trajectories of newly synthesized proteins labeled with QDs. Left, DIC and QD labeling (green); active synapses are visualized with FM4–64; right, Individual

trajectories reconstructed from QDs. Synaptic (yellow) and extrasynaptic (blue) trajectories were classified in relation to active presynaptic terminals labeled with FM4–64. Scalebar = 2μm. (**d**) Average MSD of synaptic and extrasynaptic QDs as a function of time. Values are mean ±SEM. (**e**) Cumulative distribution of newly synthesized proteins diffusion coefficients at (n=101) and outside (n=262) synapses (Kolmogorov–Smirnov test, p<0,001). The diffusion coefficients of the γ_2–$GABA_AR$ subunit at synapses (n=212) and at extrasynaptic sites (n=77) (KS test, p<0,001) were plotted for comparison. (**f**) Frequency distribution of extrasynaptic diffusion coefficients of newly synthesized proteins. Colored bars correspond to the 75% of the values (12,5%–87,5% range, black squares correspond to the mode of the distribution) of D values for AMPAR (purple, 50), $GABA_AR$ (red), mGluR5 (green, 31,32) and GFP–GPI (grey, 30). (**g**) Frequency distribution of extrasynaptic diffusion coefficients of γ_2–$GABA_AR$. The red bar on the x-axis corresponds to 75% of the values (12,5%–87,5% range) of γ_2–$GABA_AR$ diffusion coefficients.